BBA - Molecular Basis of Disease 1865 (2019) 2356–2367

Contents lists available at ScienceDirect

BBA - Molecular Basis of Disease

journal homepage: www.elsevier.com/locate/bbadis

Mutations of *GADD45G* in rabbits cause cleft lip by the disorder of proliferation, apoptosis and epithelial-mesenchymal transition (EMT)

Yi Lu[a,1], Mingming Liang[a,1], Quanjun Zhang[b], Zhiquan Liu[a], Yuning Song[a], Liangxue Lai[a,b,*], Zhanjun Li[a,*]

[a] Key Laboratory of Zoonosis Research, Ministry of Education, Institute of Zoonosis, College of Veterinary Medicine, Jilin University, Changchun 130062, China
[b] CAS Key Laboratory of Regenerative Biology, Guangdong Provincial Key Laboratory of Stem Cell and Regenerative Medicine, South China Institute for Stem Cell Biology and Regenerative Medicine, Guangzhou Institutes of Biomedicine and Health, Chinese Academy of Sciences, Guangzhou, 510530, China

ARTICLE INFO

Keywords:
GADD45G
Cleft lip
Rabbit
CRISPR/Cas9
BE4-Gam

ABSTRACT

The cleft lip with or without cleft palate (CL/P) is one of the most common congenital defects in humans. Genome-wide association studies (GWAS) have been widely used for identifying candidate genes, and different genes or chromosomal regions have shown strong evidence for the presence of causal genes in CL/P. To date, two independent GWAS have identified *GADD45G* as influencing risk for CL/P. However, there is no animal model evidence about *GADD45G* related to CL/P. Here, we reported the generation of a novel *GADD45G* mutated rabbit model by CRISPR/Cas9 and CRISPR-based BE4-Gam systems. The homozygous ($GADD45G^{-/-}$) while not heterozygous ($GADD45G^{+/-}$) pups died after birth due to severe craniofacial defects of unilateral or bilateral cleft lip (CL). Moreover, the disorder of proliferation, apoptosis and epithelial-mesenchymal transition (EMT) were also determined in the medial and lateral nasal processes (MNP and LNP) of the embryonic day 13 (E13) $GADD45G^{-/-}$ rabbits, which compared with the normal wild type (WT) rabbits. Thus, our study confirmed for the first time that loss of *GADD45G* lead to CL at the animal level and provided new insights into the crucial role of *GADD45G* for upper lip formation and fusion.

1. Introduction

Cleft lip with or without cleft palate (CL/P) is one of the most common congenital diseases in humans, with approximately 1/500 to 2500 newborns born worldwide [1,2]. Clinically, cleft lip (CL) refers to a unilateral or bilateral gap between the lateral side of the upper lip and philtrum, usually extending from the upper lip and lower jaw to the nostrils and accompanied by cleft palate [3]. Another common oral-facial cleft palate is cleft palate (CP) that appears a gap in the secondary palate and the upper lip appears to be complete. The cause of CL/P is complicated, including environmental factors and genetic factors [4]. Epidemiological studies showed monozygotic twins have strong familial aggregation and consistency, indicating a genetic predisposition to CL/P [5]. Some genome-wide association studies (GWAS) were designed using both case-control and case-parent triple study, and different genes or chromosomal regions have shown strong evidence of genes for CL/P [6–10].

Growth arrest and DNA damage 45G (*GADD45G*) is a member of *GADD45* family (the growth arrest and DNA-damage-inducible 45 family), which implicated in regulating the cellular response to stresses, DNA repair, inhibition of cell cycle and survival [11–13]. Although initially considered to be unimportant for the development of mice [14], loss of function studies revealed that *GADD45G* plays a role in gender determination through the effects on p38 MAPK and *Sry* expression [15,16]. In recent studies, several GWAS have identified *GADD45G* as a candidate CL/P-related gene [6,9,10]. Of noted, the expression of *GADD45G* in embryonic day 9.5 (E9.5) mouse embryos was also detected in the dorsal midbrain, the neural tube, the cranial and dorsal root ganglia [17]. These observations imply that *GADD45G* is possibly associated with CL/P, but it is unknown whether this

Abbreviations: CL/P, cleft lip with or without cleft palate; CL, cleft lip; EMT, epithelial-mesenchymal transition; WT, wild type; CP, cleft palate; GWAS, genome-wide association studies; FNP, frontonasal prominence; MXP, maxillary processes; MAN, mandibular processes; MNP, medial nasal process; LNP, lateral nasal process; λ, lambdoidal junction; KO, knockout; Shh, sonic hedgehog; POTS, potential off-target sequences

* Corresponding authors at: Key Laboratory of Zoonosis Research, Ministry of Education, Institute of Zoonosis, College of Veterinary Medicine, Jilin University, Changchun 130062, China.
E-mail addresses: lai_liangxue@gibh.ac.cn (L. Lai), lizj_1998@jlu.edu.cn (Z. Li).
[1] These authors contributed equally to this work.

https://doi.org/10.1016/j.bbadis.2019.05.015
Received 30 January 2019; Received in revised form 17 May 2019; Accepted 27 May 2019
Available online 29 May 2019
0925-4439/

connection is causal or accidental in animal level.

The upper face (lip and nose) of mammalian is produced by several paired and unpaired tissues during early organogenesis [18,19]. The formation of upper lip begins embryonic day 9 (E9) in the mouse, and complete by E12.5 [19]. The original mouth consists of 5 separate protrusions, the frontonasal prominence (FNP) is on the upper side, a pair of maxillary processes (MXP) are on the outside and a pair of mandibular processes (MAN) are on the lower side [19]. The FNP grows continuously and is divided into the medial nasal process (MNP) and lateral nasal process (LNP), which protrude around the nasal placodes to form the nasal pits. Around E11, fusion in the lambdoidal junction (λ) which LNP, MXP, and MNP result in the formation of the nostrils and the lip [19].

Morphogenesis and growth of the face require precise coordination of cellular programs including proliferation, differentiation, and apoptosis [20]. Interference from either developmental event can lead to facial cleft [21]. At the λ, the epithelial seam cells between fusing processes have to break down [22]. Active cell death can be observed in the epithelial seams between MNP and LNP in mice [19]. However, mice that are apoptotic due to inhibition of the caspase signaling pathway did not show CL, but secondary malformations and extracerebral malformations [23,24]. These results suggested that there are other mechanisms leading to the removal of epithelial cells. Some studies have shown that epithelial-mesenchymal transition (EMT) occurs in epithelial seam cells during facial fusion [25,26]. Additionally, *Kurosaka H* discovered that a disturbed sonic hedgehog (Shh) signaling resulted in persistent SSEA1-positive periderm cells on the MNP, which possibly led to alterations in the balance of cell proliferation and apoptosis at the epithelial seam, which caused the CL phenotype [27].

In this study, we reported that *GADD45G* genes are highly expressed at the MNP and LNP during upper lip formation and fusion in rabbits. By generating rabbit deficient for *GADD45G* gene, we demonstrated that loss of *GADD45G* results in CL at the animal level. Furthermore, the increased cell proliferation, while reduced cell apoptosis and EMT at λ of E13 *GADD45G*$^{-/-}$ rabbits, which will lead to the persistence of the seam in the MNP and LNP and pathogenesis of CL. Altogether, these data provided the first direct evidence that *GADD45G* is a genetic risk factor for CL.

2. Materials and methods

2.1. Ethics statement

New Zealand rabbits were obtained from the Experimental Animal Center of Jilin University (Changchun, China). All rabbit-related experiments were conducted in accordance with the experimental specifications and standards approved by the Jilin University Animal Care and Use Committee guidelines.

2.2. CRISPR/Cas9-mediated GADD45G gene knockout (KO) in rabbits

The sgRNAs targeting *GADD45G* were designed, assembled and in vitro transcribed as previously described [28]. The sgRNA oligonucleotides were annealed and inserted into the pUC57-Simple-gRNA vector (Addgene ID 51306) as described [29]. The pSpCas9 (PX165) vector was obtained from Addgene (#48137). The protocol for microinjection and embryo transfer has been described in our previously published data [30]. Briefly, a mixture mRNA of Cas9 (200 ng/μl) and sgRNA (50 ng/μl) was co-injected into the cytoplasm of rabbit zygotes and then transferred into the recipient rabbits.

2.3. BE4-Gam-mediated base editing in rabbit GADD45G

The BE4-Gam sgRNA was designed, assembled and in vitro transcribed as previously described [31]. The BE4-Gam vector was obtained from Addgene (#100806). The protocol for microinjection and embryo transfer has been described [31].

2.4. Mutation detection and off-target analysis

Mutation detection was performed as previously described [32]. The PCR primers for the sgRNA target sites were as follows: forward, 5′-ACCCCGACAATGTGACCTTC-3′ and reverse, 5′-ACCACGTCGATCAG ACCAAG-3′ (fragment size of *GADD45G*-KO allele: 447 bp), forward, 5′-GAAGCTTGCCGGAGCAG-3′ and reverse, 5′-TCACACGTTCAGGACT TTGG-3′ (fragment size of *GADD45G* (p.Q36Stop) allele: 253 bp). The T-clones were sequenced and analyzed using BLAST and SnapGene.

Potential off-target sequences (POTS) were predicted to analyze according to the CRISPR Design Tool (http://crispr.mit.edu/) and Cas-OFFinder (http://www.rgenome.net/cas-offinder/) [33]. The PCR products were subjected to T7EI assay and Sanger sequencing.

2.5. Scanning electron microscopy

The E13 and E15 rabbit embryos were fixed in 4% glutaraldehyde in PBS at 4 °C. Specimens were washed with PBS, dehydrated in ethanol series, dried in carbon dioxide and sprayed with gold, then observed under an electron microscope (Hitachi, Tokyo, Japan) at 10 kV accelerating voltage [34]. E13 and E15 were determined as the timing of upper lip and facial development by obtaining rabbit embryos of different days (E11–E16).

2.6. Histological examination and immunostaining

The E13 rabbit embryos were fixed in 4% paraformaldehyde (PFA) and processed into paraffin-embedded serial sections. Hematoxylin and Eosin (H&E), immunohistochemical were performed as described previously [35,36]. The antibody used for immunohistochemistry was Anti-GADD45G antibody [2F12] (Abcam, ab140378; 1:150). The stained sections were imaged with a microscope (Nikon, Tokyo, Japan).

For proliferation analysis, we performed immunostaining of phospho-histone H3 (pH 3) (Abcam, ab14955; 1:200). PH3-positive cells and a total number of cells were quantitated in three randomly selected sections from each experimental group. Apoptosis assays were performed using caspase-3 (active) immunostaining (Beyotime, AF1150; 1:200) according to the manufacturer's protocol. Sections were counterstained with DAPI. Meanwhile, detection of apoptotic cells in TdT-mediated dUTP nick-end labeling (TUNEL) assay using an in situ cell death assay kit (Roche Applied Science, Upper Bavaria, Germany). EMT assays were performed using E-Cadherin Mouse Monoclonal Antibody (Beyotime, AF0138; 1:200) and Vimentin Mouse Monoclonal Antibody (Abacam, ab8978; 1:1000). Images were captured using a laser scanning confocal microscope (Olympus, Tokyo, Japan) [36].

2.7. Real-time quantitative PCR (q-PCR)

q-PCR was performed as described previously [28]. Briefly, total RNA was extracted from MNP and LNP of WT and E13 *GADD45G*$^{-/-}$ embryos using Trizol (Tiangen, Beijing, China) and reverse-transcribed to cDNA using PrimeScript RT Master Mix (TaKaRa, Tokyo, Japan). The q-PCR primers were as follows: *GADD45G* forward, 5′-CAGATCCACTT CACGCTGAT-3′ and *GADD45G* reverse, 5′-CCACGTCGATCAGACC AAG-3′, *GAPDH* forward, 5′-TCCATTCATTGACCTCCACTAC-3′, and *GAPDH* reverse, 5′-GACCAGCTTCCCGTTCTC-3′. q-PCR was performed with TB Green *Premix Ex Taq* II (TaKaRa, Japan) and *GAPDH* was used as internal control.

2.8. Western blotting

RIPA buffer (Beyotime, Shanghai, China) supplemented with 0.01% PMSF (BOSTER, Wuhan, China) was used for total protein extraction from ear and λ region tissues of E13 rabbit embryos. The proteins were

separated by 12% SDS-PAGE gel, transferred onto nitrocellulose filter membrane (NC) membranes. Then blocked and incubated with primary antibodies for Anti-GADD45G antibody [2F12] (Abcam, ab140378; 1:150) and β-actin (Beyotime, AA128; 1:1000). Subsequently, the membranes were probed with secondary antibody (Beyotime, A0216; 1:1000). The membranes were visualized by the ECL Plus Western Blotting System (Beyotime, Shanghai, China). The intensity was measured using Image J software (NIH, USA).

The 3 D structure models of the WT and *GADD45G* mutant proteins were built from their amino acid sequences according to the web site: http://swissmodel.expasy.org/ [37].

2.9. Statistical analysis

Data are expressed as mean ± SEM, with at least three individual determinations in all experiments. Data of two group comparisons were determined by unpaired Student's *t*-test and multiple group comparisons were analyzed with one-way ANOVA with Bonferroni's post-tests using Prism 6.0 (GraphPad Software). $p < 0.05$ was considered statistically significant. The origin of these embryonic mutant animals which for analysis of morphology, proliferation, apoptosis and gene expression were derived from the F1 heterozygous G1-2 embryos by mating and the tail tissues were collected for mutation detection.

3. Results

3.1. CRISPR/Cas9-mediated GADD45G knockout (KO) leads to CL in rabbits

To date, GWAS have identified *GADD45G* as a candidate CL/P-related gene [6,9,10]. At present, due to the high conservation of orofacial development between humans and rodent, the mouse has been widely used as an effective model to study orofacial development and defects [38,39]. Although the rabbit has mainly been used as a surgical model for creating and repairing clefts currently, the rabbit shares more similarities with humans in terms of physiology, anatomy and genetics than the mouse [40,41].

Firstly, we designed a pair of sgRNAs targeting Exon 2 and Exon 3 of *GADD45G* in rabbit (Fig. 1A). In order to test the efficiency of gene KO of *GADD45G* in zygotes, a mixture mRNA of Cas9 and sgRNAs were co-injected into the rabbit zygotes and cultured rabbit zygotes to the blastocyst stage. As shown in Supplementary Table S1, 78.4% ± 6.7 of injected embryos ($N = 154$) developed to the blastocyst stage and 76.3% ± 3.9 carried mutations in *GADD45G* at the target sites. There was no significant difference in the developmental rate between the non-injected embryos and microinjected embryos ($p < 0.05$). These results demonstrated that the CRISPR/Cas9 system is efficient for targeting the *GADD45G* gene in rabbit zygotes.

To generate *GADD45G* KO rabbit, 60 injected zygotes were transferred into two surrogate rabbits and produce 11 live pups (Supplementary Table S2). As shown in Figs. 1B and S1, 10 of 11 newborn pups carried homozygous *GADD45G* mutations ($GADD45G^{-/-}$). In addition, genotype data indicated that 50% of F0 rabbits had the *GADD45G* mosaicism (#3, #4, #6, #7 and #11), revealing that CRISPR generated mosaicism was commonly detected in F0 generation (Fig. S1) [32,42–44]. To examine the off-target effects in these $GADD45G^{-/-}$ rabbits, we detected the top 10 potential off-target sites of the PCR products using Sanger sequencing and the T7E1 assay. The primers for the off-target assay are listed in Supplementary Data 1. The results showed there are no off-target mutations at these potential sites in the *GADD45G KO* rabbits (Fig. S3).

Of noted, all $GADD45G^{-/-}$ rabbits died within three days of birth and exhibited unilateral (10%) or bilateral (90%) cleft lip (CL) at the postnatal 3 days (P3) (Fig. 1C, D, and G). Usually, the CL is often accompanied by cleft palate (CP) [27,45,46], which geometrically divided into four (anterior, middle, posterior and posterior end) regions along the anterior-posterior (AP) axis [47–49]. In this study, there is no evidence of CP in these $GADD45G^{-/-}$ rabbits (Fig. 1E and F). Furthermore, the $GADD45G^{-/-}$ rabbit pups with unilateral or bilateral CL could not suck the pacifier normally (Movies 1, 2 and 3). Thus, it was speculated that the cause of early death in $GADD45G^{-/-}$ rabbits was from suck problem, which is also the severe problem of the infancy with CL in clinical [50].

3.2. Generation of GADD45G (p.Q36Stop) rabbit using the BE4-Gam system

Although CRISPR/Cas9 is expected to be the gene editing tool, the significance of targeted mutations, such as the large deletions and more complex genomic rearrangements caused by DSBs have also been reported in the previous study [51]. Recently, a programmable cytidine deaminase based on the CRISPR/Cas9 system has been shown to convert from C-to-T (BE4-Gam system) [52] without generating DSBs [31]. To further confirm the role of *GADD45G* in craniofacial morphogenesis, a single C-to-T conversion was designed to generate a premature stop codon (p.Q36stop) in exon 1 of rabbit *GADD45G* (Fig. 2A). This mutation would inactivate the gene by directly converting the normally coded codons to a STOP codon.

To test the efficiency of BE4-Gam-mediated base editing of *GADD45G* in zygotes, a mixture BE4-Gam mRNA and sgRNAs were co-injected into the rabbit zygotes and cultured rabbit zygotes to the blastocyst stage. As shown in Supplementary Table S3, 77.6% ± 9.8 of injected embryos ($N = 152$) developed to the blastocyst stage and 76.1% ± 6.3 carried p.Q36stop in *GADD45G* at the target sites. These results demonstrated that the BE4-Gam system is efficient for the generation of p.Q36stop in the *GADD45G* gene in rabbit zygotes.

In order to generate *GADD45G* (Q36Stop) rabbits, 52 injected zygotes were transferred into two surrogate rabbits (Supplementary Table S4) and produced 8 live pups. The base editing was determined by Sanger sequencing of the PCR products. As shown in Fig. 2B, a single C-to-T conversion yield a premature stop codon (p.Q36Stop) in the gRNA-target region was determined in all pups (100%). The result from Sanger sequencing and EditR [53] also demonstrated the efficient C-to-T conversion in the *GADD45G* (Q36Stop) rabbit (Fig. 2C and D). As expected, 7 of 8 (87.5%) *GADD45G* (p.Q36stop) rabbits, except the G1-2, exhibited bilateral CL (Fig. 2E and G), and all of the *GADD45G* (P.Q36stop) rabbits with CL died within 3 days of birth due to the sucking problem (Fig. 2F). Furthermore, no off-target mutations were detected at the 22 potential off-target sites in the *GADD45G* (p.Q36stop) rabbits (Fig. S4). The primers for the off-target assay are listed in Supplementary Data 2.

3.3. No CL in the heterozygous GADD45G (p.Q36stop) rabbits

Due to the high efficiency of CRISPR/Cas9 and BE4-Gam system, there are no heterozygous *GADD45G* mutated ($GADD45G^{+/-}$) rabbits (Figs. S1 and S2), which limited the CL phenotype determination of $GADD45G^{+/-}$ rabbits. Luckily, the G1-2 *GADD45G* (p.Q36stop) rabbit without CL and could be survived to sex maturation (Fig. 3A and B). We hypothesize this is due to mosaicism mutation from microinjection [54], which have been widely observed in zebrafish [55], mice [56] and *Drosophila* [57] when using CRISPR based gene editing system.

To determine whether the heterozygous *GADD45G* (p.Q36stop) rabbits ($GADD45G^{+/-}$ rabbits) would be CL, female G1-2 rabbit was mated with WT male New Zealand rabbits and gave birth to 5 live pups. The Sanger Sequencing results showed that the heterozygous *GADD45G* (p.Q36stop) mutation was determined in all pups, while there is no CL in those $GADD45G^{+/-}$ rabbits (Fig. 3C and D). However, it is possible that there might be modifier mutations present in G1-2 that could alter the clefting rate. Therefore, by intercrossing the F1 heterozygotes, we obtained $GADD45G^{-/-}$ rabbits with cleft lip and $GADD45G^{+/-}$ rabbits without cleft lip. This further confirmed that there is no cleft lip in the

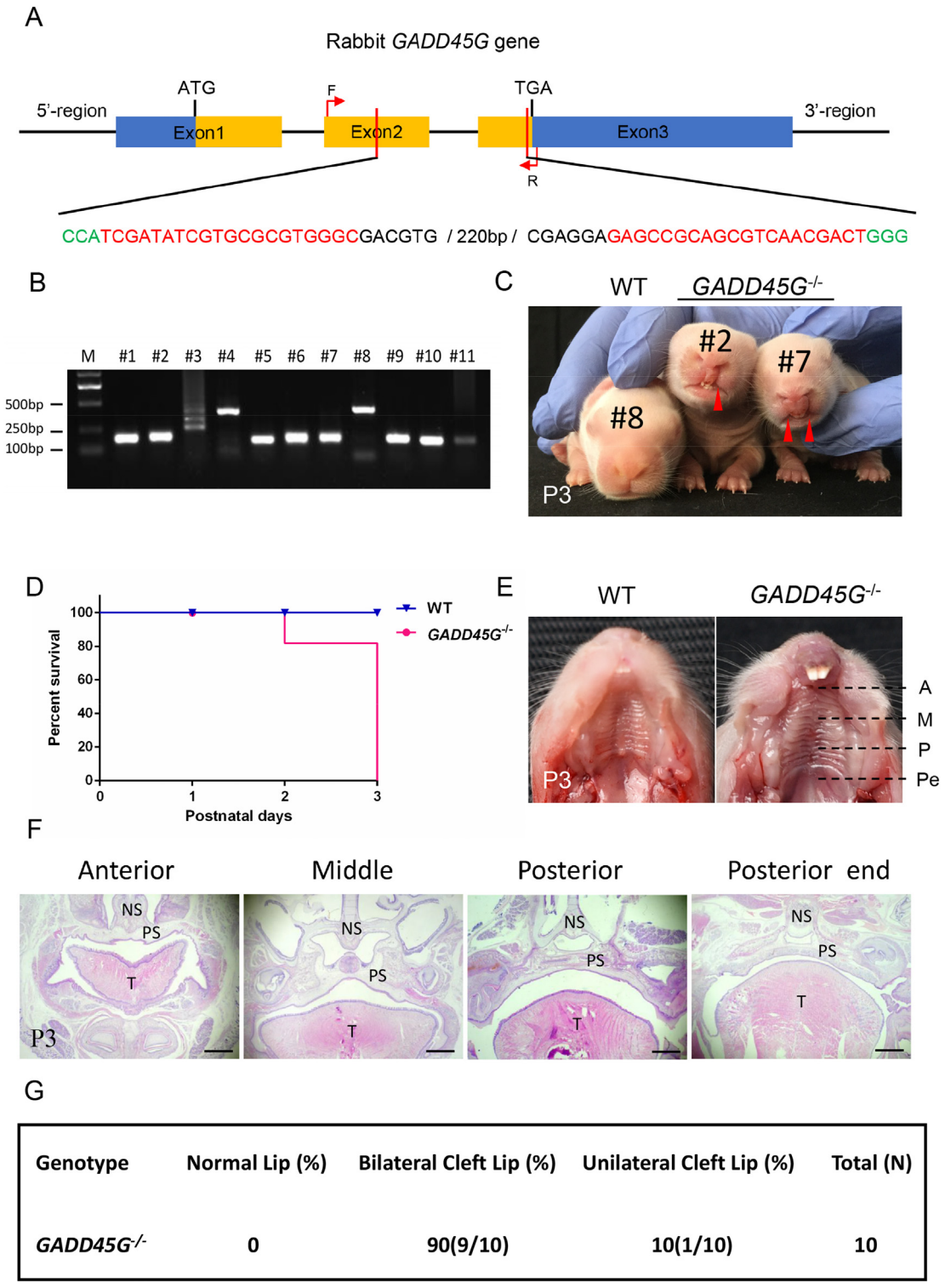

Genotype	Normal Lip (%)	Bilateral Cleft Lip (%)	Unilateral Cleft Lip (%)	Total (N)
GADD45G$^{-/-}$	0	90(9/10)	10(1/10)	10

Fig. 1. Generation of *GADD45G* KO rabbits using CRISPR/Cas9 system.
(A) Schematic diagram of two sgRNA target sites located in exon 2 and exon 3 of the rabbit *GADD45G* locus. The CDS (sequence coding for aminoacids in protein) of *GADD45G* is indicated by orange boxes; target sites of the two sgRNA sequences (sgRNA1 and sgRNA2) are highlighted in red, protospacer-adjacent motif (PAM) sequences are highlighted in green. Primers F and R were used for mutation detection. (B) Mutation detection by PCR in pups #1–#11. M, the DNA ladder (DL2000). #1–#11, the *GADD45G* mutated rabbit pups. (C) Photographs of *GADD45G*$^{-/-}$ rabbits have unilateral or bilateral cleft lip (CL) (red arrows) at the postnatal 3 days (P3). (D) Kaplan–Meier survival curves for the *GADD45G*$^{-/-}$ and WT rabbits (E) Inferior view of palatal shelves of P3 *GADD45G*$^{-/-}$ and WT rabbit. Dotted lines indicate the equivalent position of coronal sections; A, anterior; M, middle; P, posterior; Pe, posterior end. (F) H&E-stained coronal sections of P3 rabbit pup head showing anterior, middle, posterior, and posterior end regions. NS, nasal septum; T, tongue; PS, palatal shelves. (G) Distribution of CL in *GADD45G*$^{-/-}$ rabbits is shown as a percentage of mutants that exhibit normal lip or CL over the total number of mutants analyzed. WT: wild type control. Scale bars: 1 mm (panel F). (For interpretation of the references to color in this figure legend, the reader is referred to the online version of this chapter.)

A

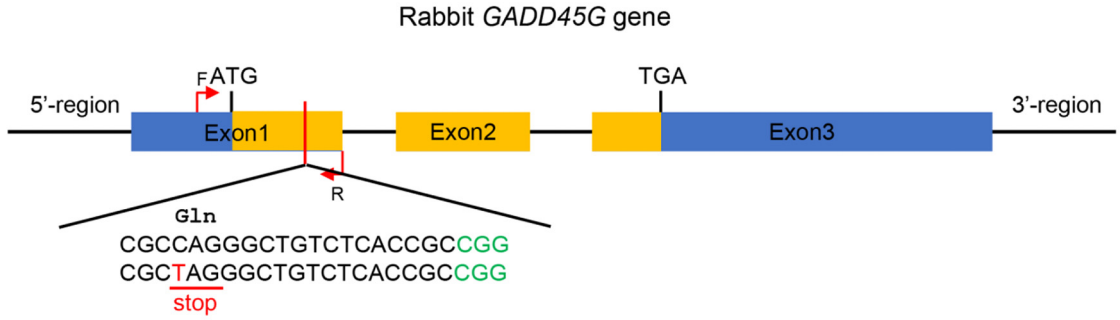

B

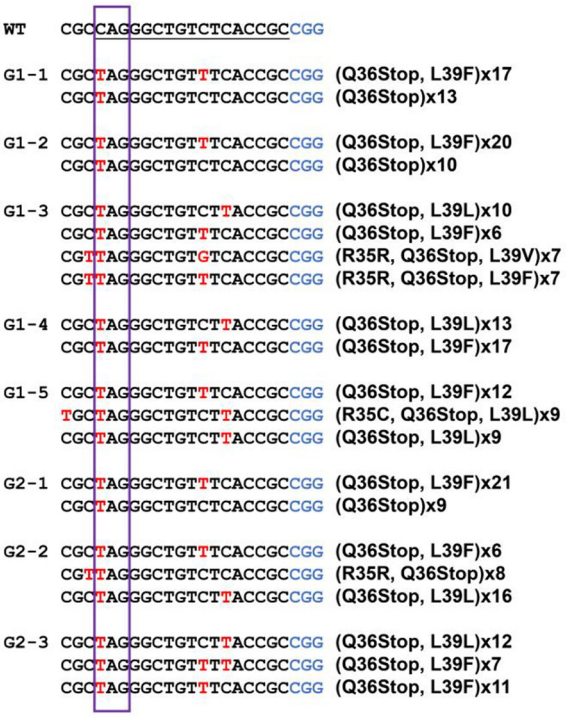

C

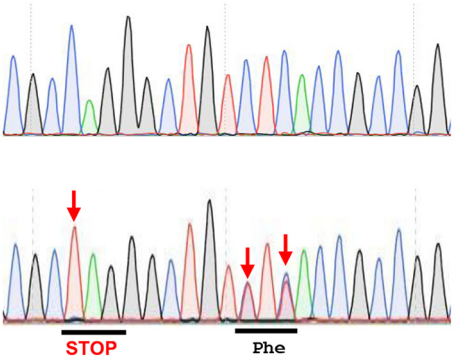

D

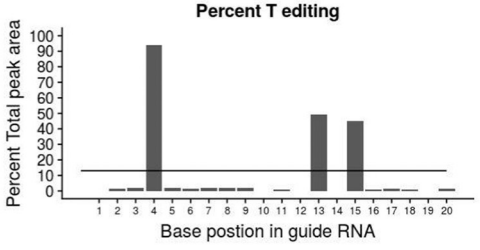

E

F

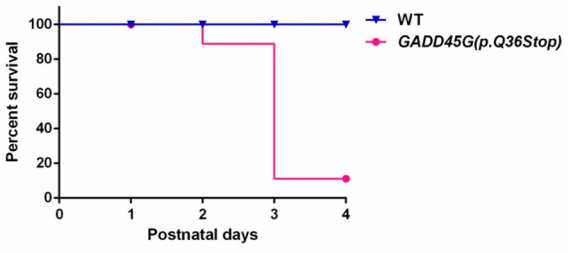

G

Genotype	Normal Lip (%)	Bilateral Cleft Lip (%)	Unilateral Cleft Lip	Total (N)
GADD45G(p.Q36Stop)	12.5(1/8)	87.5(7/8)	0	8

(caption on next page)

Fig. 2. Generation of *GADD45G* (p.Q36Stop) rabbit model using the BE4-Gam system.
(A) The target sequence within the *GADD45G* locus. Target sequence (black), PAM region (green), CDS region (orange) and substituted nucleotide (red, C = T). Relevant codon identities at the target site are presented beneath the DNA sequence. Primers F and R were used for mutation detection. (B) PCR amplicons of the target site from genomic DNA of mutant rabbits were subcloned into the pGM-T vector and sequenced. The number of clones for each sequence pattern is indicated. Target sequence (underlined), PAM region (blue), and substituted nucleotide (red). A purple box indicates the termination codon. (C) Sanger sequencing chromatograms of DNA from WT and *GADD45G* (p.Q36Stop) rabbits (G1-4). The red arrow indicates the substituted nucleotide. Relevant codon identities at the target site are presented beneath the DNA sequence. (D) The predicted editing bar plot based on Sanger sequencing chromatograms from G1-4 by EditR. (E) *GADD45G* (p.Q36Stop) rabbits exhibited a bilateral cleft lip (red arrows) at P3. (F) Kaplan–Meier survival curves for the *GADD45G* (p.Q36Stop) and WT rabbits. (G) Distribution of CL in *GADD45G* (p.Q36Stop) mutants, is shown as a percentage of mutants that exhibit normal lip or CL over the total number of mutants analyzed. (For interpretation of the references to color in this figure legend, the reader is referred to the online version of this chapter.)

heterozygous *GADD45G* rabbits (Figs. 3E and S5). In addition, the predicted 3D models showed the disrupted *GADD45G* protein structure (Fig. 3F), which is also confirmed by Western blotting. As shown in Fig. 3G and H, the GADD45G protein was reduced significantly in $GADD45G^{+/-}$ rabbits while completely loss of expression in $GADD45G^{-/-}$ rabbits, which compared to WT rabbits ($p < 0.01$).

3.4. GADD45G is required for upper lip formation and fusion

Previously study showed the high expression of *GADD45G* in the dorsal midbrain, the neural tube, the cranial and dorsal root ganglia of E9.5 mouse embryos [17]. Meanwhile, the formation of the upper lip begins at E9.5 of mouse embryogenesis [19], imply the *GADD45G* may have roles on the lip formation and fusion. In addition, the upper lip is formed by the synergistic outgrowth and fusion of MXP with LNP and MNP [58]. Thus, we examined the craniofacial morphology of $GADD45G^{-/-}$ rabbit at day 3 of partum (P3) by H&E staining. The result showed the disrupted fusion of the premaxillary and lateral walls of the lips, bilateral clefts of the upper lip region (black dashed box), and the absent hair follicles (black arrow) in the $GADD45G^{-/-}$ rabbits (Fig. 4A).

To further investigate whether the *GADD45G* is required for upper lip formation and fusion, the scanning electron microscopy and immunohistochemistry (IHC) were performed between the embryos day 13 (E13) WT and $GADD45G^{-/-}$ rabbits. The scanning electron microscopy confirmed bilateral clefts of the upper lip region, LNP and MNP are obviously underdeveloped, and the MNP failed to extend to the LNP in E13 $GADD45G^{-/-}$ rabbits (white arrow). In addition, E15 $GADD45G^{-/-}$ embryos showed a clear fully bilateral CL (white dashed box), which compared to the normal development WT rabbits (Fig. 4B). Furthermore, IHC result confirmed the high expression of *GADD45G* in the epithelium versus the mesenchyme of the MNP and LNP WT E13 rabbits, while no expression in the $GADD45G^{-/-}$ rabbits (Fig. 4C). This result was also confirmed by the q-PCR, revealed the significantly decreased *GADD45G* expression in the $GADD45G^{-/-}$ rabbits ($p < 0.001$) (Fig. 4D).

Thus, the results indicate that *GADD45G* plays a key role in the formation and fusion of the upper lip by regulating the outgrowth of the facial processes and/or the fusion between the MNP and LNP.

3.5. Increased cell proliferation and reduced EMT in the MNP and LNP of $GADD45G^{-/-}$ embryo

Extensive studies have shown the important role of cell proliferation and EMT in craniofacial development [20,25,34,59]. Thus, the cell proliferation and EMT between the E13 WT and $GADD45G^{-/-}$ embryos were compared analysis using phospho-histone H3 (PH3), E-cadherin and Vimentin staining, respectively. The IHC result shown the significantly increased mitotic cells (PH3 positive) in the MNP and LNP of E13 $GADD45G^{-/-}$ embryos ($p < 0.01$), which compared with the E13 WT embryos (Fig. 5A and B). In addition, immunostaining for the E-cadherin showed E-cadherin significantly increased within the λ epithelia (white dashed line) in E13 $GADD45G^{-/-}$ embryos (red staining) (Fig. 5C), and immunostaining for the Vimentin showed the Vimentin significantly decreased within the mesenchyme (white dashed line) in E13 $GADD45G^{-/-}$ embryos (green staining) (Fig. 5D). These results suggest that the increased cell proliferation and decreased EMT is associated with the failure of lip fusion in the E13 $GADD45G^{-/-}$ embryos.

3.6. Reduced apoptosis in the MNP and LNP of $GADD45G^{-/-}$ embryo

Multiple cellular processes occur at λ including apoptosis, mediate removal of epithelial cells at the seams [19,20,60]. Apoptosis ensures that sufficient cell numbers are removed from the epithelial seam to promote adhesion of the intermediate process of convergence and occurs before and during the fusion in the MNP and LNP [19]. Thus, to determine whether the abnormal apoptosis in the $GADD45G^{-/-}$ embryos, we performed cleaved caspase-3 immunofluorescence (IF) and TUNEL staining between the E13 WT and $GADD45G^{-/-}$ rabbits. As shown in Fig. 6B and D, the reduced apoptosis in the MNP and LNP were determined in the E13 $GADD45G^{-/-}$ embryos, which compared with the E13 WT embryos ($p < 0.05$). Moreover, we detected apoptotic cells at the seams in controls, but not in $GADD45G^{-/-}$ embryos. Interestingly, we found the apoptotic cells are regularly arranged on the LNP and MNP (white dashed line) in the WT E13 embryo, while disorderly arrangement in the E13 $GADD45G^{-/-}$ embryos (Fig. 6A and C). These results indicated that the reduced apoptosis in epithelial seams during upper lip morphogenesis in the E13 $GADD45G^{-/-}$ embryos.

Taken together, these results suggested that the loss of *GADD45G* leads to the increased cell proliferation while reduced EMT and apoptosis in the MNP and LNP, which ultimately leads to the occurrence of CL in the $GADD45G^{-/-}$ embryo (Fig. 6E).

4. Discussion

Although the *GADD45G* has been identified as a candidate CL/P-related gene [6,9,10], a direct demonstration of a link between *GADD45G* and CL/P has not been reported. In this study, by inactivate *GADD45G* in the rabbits, we provide the first direct animal model evidence of *GADD45G* function in upper lip formation and fusion. These rabbits exhibited CL and all died within three days due to sucking problem. Although previous studies demonstrated that *GADD45G* is not necessary for embryonic development except sex determination [14–16,61], these may be attributed to a difference in genetic background between the mice and rabbits.

In this study, we first generated *GADD45G* KO rabbits via injection of Cas9 mRNA and a pair of sgRNAs targeting exon 2 and exon 3 of the *GADD45G* gene and demonstrated the *GADD45G* KO rabbits exhibited CL. However, off-target effects are a major problem in the Cas9-mediated gene editing system [62,63]. Recently, the cytosine base editors (CBEs) and adenine base editors (ABEs) systems have been developed that directly perform nucleotide conversion without introducing double-stranded breaks (DSB) and low off-target effect [64,65]. Thus, both the CRISPR/Cas9 and BE4-Gam were used for the mutation of *GADD45G* gene in this study. These results confirmed that our animal level results are specifically due to the mutation of *GADD45G* while not off-target effects. Additionally, the functional domains of the GADD45G protein were predicted using a web resource (http://smart.embl.de) [66], which shown there is only a Ribosomal_L7Ae domain in the

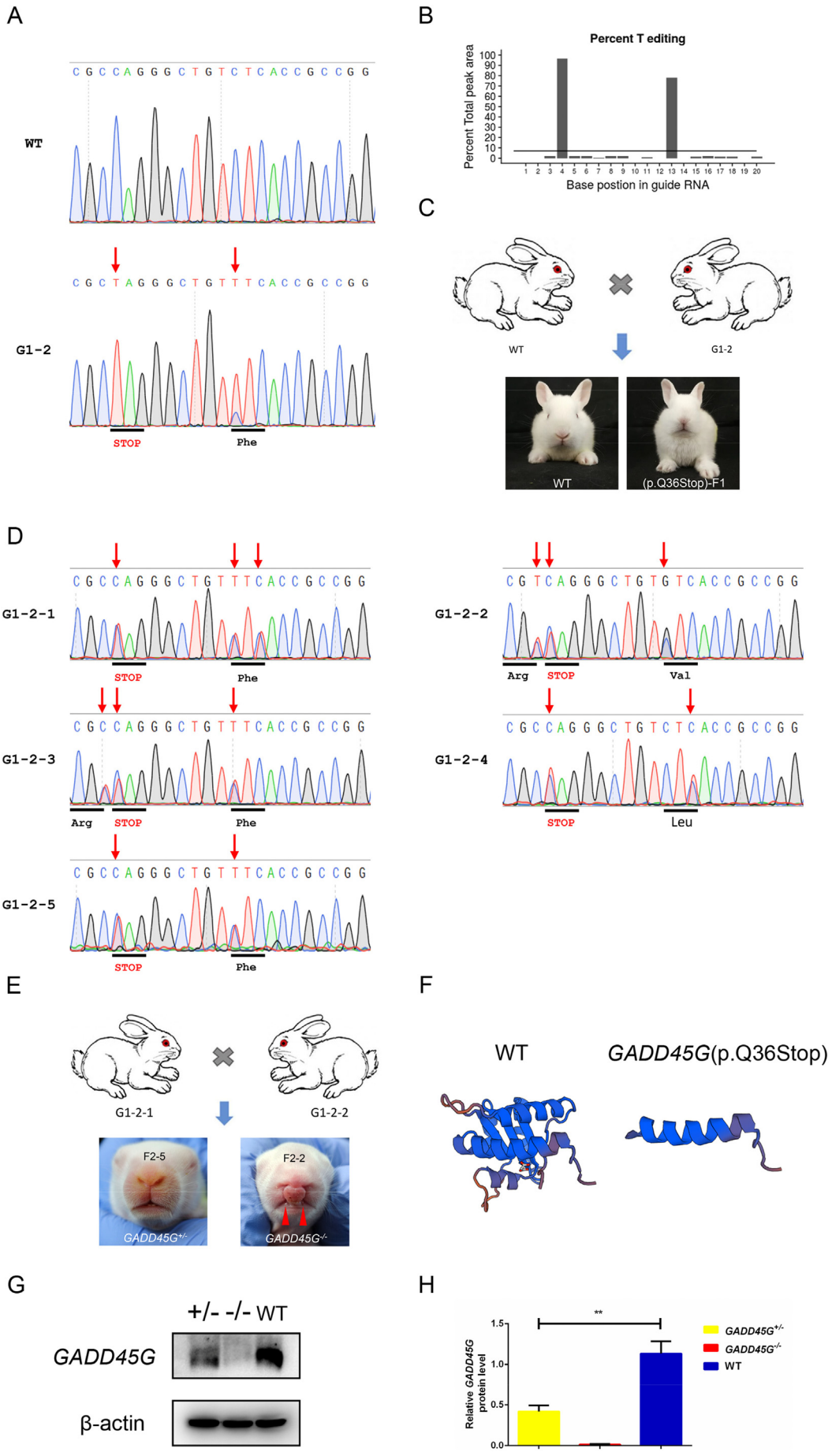

(caption on next page)

Fig. 3. No CL in the heterozygous *GADD45G*$^{+/-}$ rabbits.
(A) Sanger sequencing chromatograms of DNA from WT and *GADD45G* (p.Q36Stop) rabbits (G1-2). The red arrow indicates the substituted nucleotide. Relevant codon identities at the target site are presented beneath the DNA sequence. (B) The predicted editing bar plot based on Sanger sequencing chromatograms from G1-2 by EditR. (C) A male rabbit (WT) was mated with female rabbits (G1-2) and there is no CL in these F1 pups. (D) Sanger sequencing chromatograms of DNA from F1 pups. The red arrow indicates the substituted nucleotide. Relevant codon identities at the target site are presented beneath the DNA sequence. (E) Female G1-2-2 rabbit was mated with male G1-2-1 rabbit and there is no cleft lip in the heterozygous *GADD45G* rabbits. (F) Computer modeling the 3D structure between the WT and *GADD45G* (p.Q36Stop). (G) Western blotting from the ear tissue of the *GADD45G* gene mutant rabbits. Equal amounts of protein were used and β-actin was the internal control. (H) Grey-scale analysis of the Western blotting result by ImageJ software. Error bars represent ± SEM. $^{**}p < 0.01$. (For interpretation of the references to color in this figure legend, the reader is referred to the online version of this chapter.)

GADD45G protein (Position:24 to 113), and both the CRISPR/Cas9 and BE4-Gam mediated gene mutation will destroy this domain and affect its activity.

To date, a number of genetic mutate model animals have been generated to study human cleftings, such as *Irf6*, *p63*, *Wnt* and *Bmp* genes [46,67–69]. Although clefts of the secondary palate occur frequently in transgenic or knockout animal embryos, isolated CL animal model is very rare [70–72]. In comparison with WT rabbits, *GADD45G* mutant rabbits exhibited CL without CP. Thus, this model provides one of the few, CL without CP animal models for craniofacial disease and provides us to better understand and study the different aspects of the development of the lips and palate during the embryonic period. Additionally, by mating G1-2 mosaic female rabbit with wild males and intercrossing the F1 heterozygotes, we found no CL in the heterozygous *GADD45G* (p.Q36stop) rabbits. Therefore, we hypothesize that *GADD45G* is a recessive gene in CL. Likewise, common CL genes such as IRF6, Lrp6, and patched1 are recessive genes in CL [34,60,73].

Previous studies have shown that face morphogenesis requires the precise coordination of procedures including proliferation, differentiation, and apoptosis [20]. We have investigated the link between EMT and lip development using a mutant of *GADD45G* in the Embryonic period. E13 *GADD45G*$^{-/-}$ embryos exhibited E-cadherin protein was

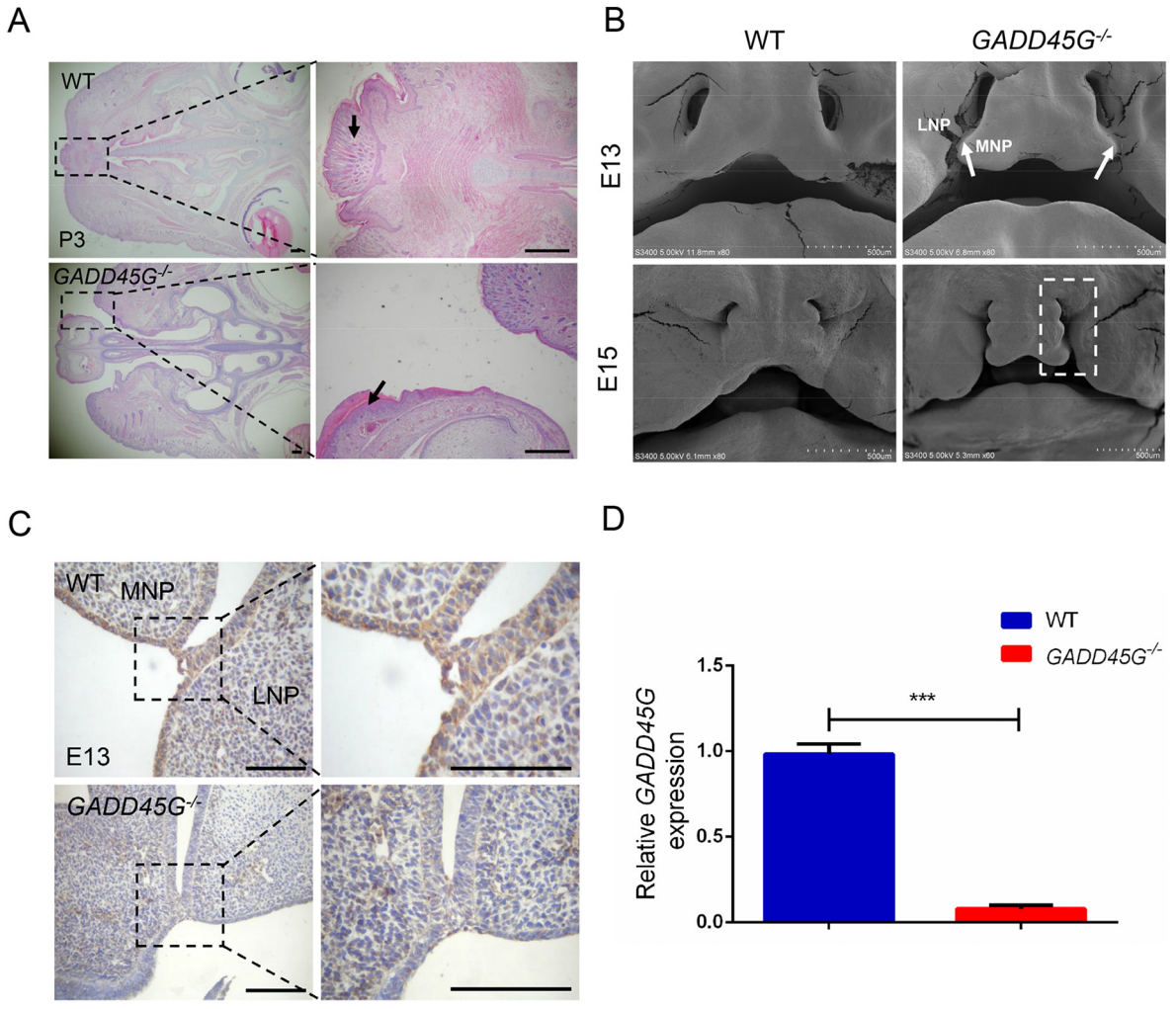

Fig. 4. *GADD45G* is required for upper lip formation and fusion.
(A) A transverse midfacial region was observed in P3 WT and *GADD45G*$^{-/-}$ rabbits by H&E staining. *GADD45G*$^{-/-}$ rabbits with bilateral clefts of the lip and lack of hair follicles in the premaxillary region (black arrows). (B) *GADD45G* gene is required for midfacial formation. Scanning Electron Microscopy (SEM) of E13 and E15 rabbit embryos. *GADD45G*$^{-/-}$ rabbits exhibit cleft lip (white dashed box). White arrowheads indicate defective fusion at the LNP/MNP fusion site. (C) Immunohistochemistry (IHC) reveals *GADD45G* is highly expressed in the epithelium of LNP and MNP and the mesenchyme of E13 embryos. (D) q-PCR confirmed the high *GADD45G* expression in λ of E13 embryos. *GAPDH* was used as a loading control. Three samples were analyzed. Error bars represent ± SEM. $^{***}p < 0.001$. $N = 3$ biologically independent samples. Scale bars: 100 μm (panels A and C).

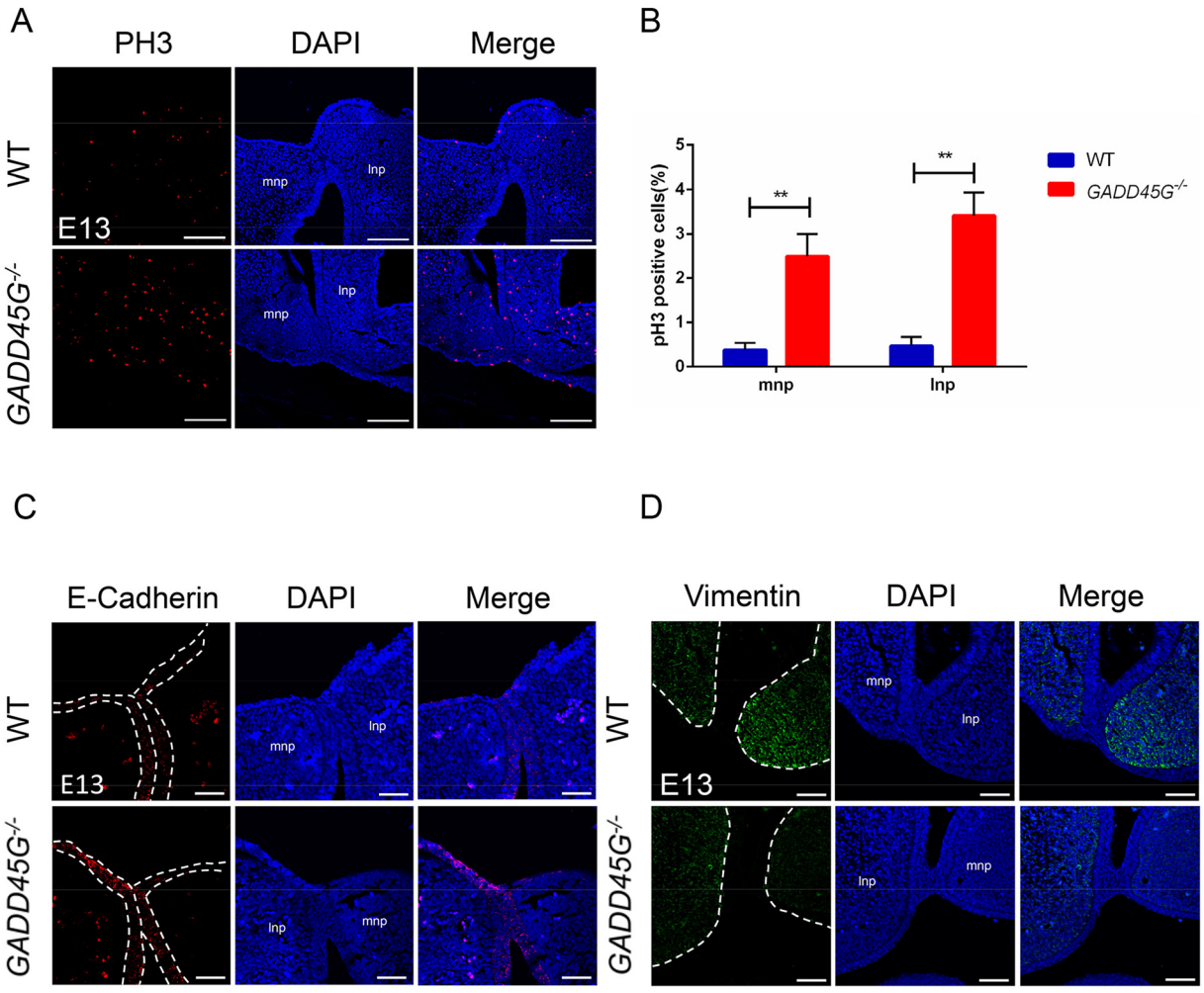

Fig. 5. Increased cell proliferation and reduced EMT in the MNP and LNP of E13 *GADD45G*$^{-/-}$ embryo.
(A) Phosphorylated histone H3 (PH3) staining shows increased cell proliferation in LNP and MNP of E13 *GADD45G*$^{-/-}$ rabbit embryos. (B) Comparison of percentage of cell proliferation in the designated area in the control and E13 *GADD45G*$^{-/-}$ rabbit embryos. (C) Immunofluorescence (IF) shows low E-cadherin in WT controls; conversely, high E-cadherin at the mutant λ points (white dashed line) of E13 *GADD45G*$^{-/-}$ rabbit embryos. (D) Immunofluorescence (IF) shows high vimentin in WT controls; conversely, low vimentin of E13 *GADD45G*$^{-/-}$ rabbit embryos. $N = 3$ biologically independent samples. Scale bars: 100 μm. $^{**}p < 0.01$.

increased significantly compared to WT within the λ epithelia, and Vimentin protein was decreased significantly compared to WT within the mesenchyme. These are consistent with others who have pointed out that the transformation of seam epithelia into mesenchyme through the process of EMT is critical to lip fusion [20,25,26]. Therefore, the aberrant EMT seen in the *GADD45G* mutant is likely to be in part responsible for CL. Furthermore, *GADD45G*$^{-/-}$ embryos showed reduced epithelial cell death and increased cell proliferation in MNP and LNP. We postulate that the balance between cell proliferation and cell death was broken, resulting in the persistent epithelial seam. Our work is consistent with other studies show that the persistence of epithelial seam is a result of decreased cell death and increased proliferation associated with CL/P [45,58,60]. Moreover, we were surprised to find apoptotic cells are regularly arranged on the mesenchymal edge of LNP and MNP at E13 (Fig. 6A and C). This phenomenon may be related to the migration of cells during lip fusion, and the underlying mechanism of this observation remains to be explored.

To the best of our knowledge, this is the first animal level report of CL caused by *GADD45G* mutant in the rabbits. Additionally, the current study provides evidence that the *GADD45G* is required for cell proliferation, EMT and apoptosis of LNP and MNP, which is essential for upper lip formation and fusion.

Supplementary data to this article can be found online at https://doi.org/10.1016/j.bbadis.2019.05.015.

Transparency document

The Transparency document associated with this article ca be found, in online version.

Declaration of Competing Interest

The authors declare no competing interests.

Acknowledgments

The authors thank Peiran Hu for providing excellent technical assistance at the Embryo Engineering Center.

Funding

This study was financially supported by the National Key Research and Development Program of China Stem Cell and Translational Research (2017YFA0105101), the Program for Changjiang Scholars and Innovative Research Team in University (No. IRT_16R32), the Strategic Priority Research Program of the Chinese Academy of Sciences

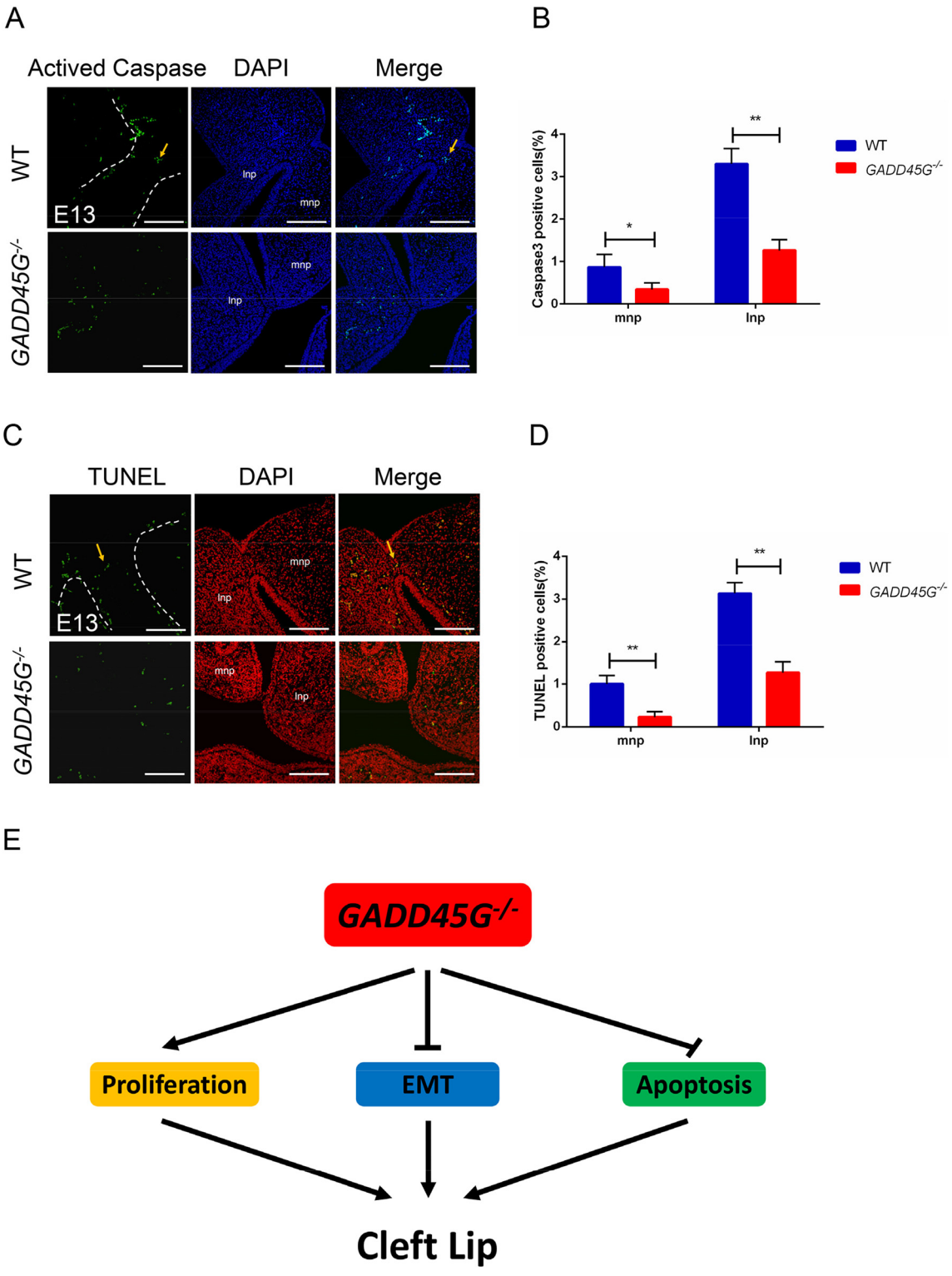

Fig. 6. Reduced apoptosis in the MNP and LNP of *GADD45G*$^{-/-}$ embryo.
(A) Activated anti-caspase 3 showing localized apoptosis on the edge of LNP and MNP (white dashed line) in control WT while reduced apoptosis at λ of E13 *GADD45G*$^{-/-}$ embryos. Meanwhile, activated anti-caspase 3 showing localized apoptosis cells at the seams in controls, but not in the *GADD45G*$^{-/-}$ embryos (orange arrow in inset). (B) Comparison of percentage of caspase3 positive cells in the designated area of λ in the WT control and E13 *GADD45G*$^{-/-}$ embryos. (C) TUNEL staining shows that cell death is significantly reduced in λ of *GADD45G*$^{-/-}$ embryos at E13. (D) Quantification of the number of TUNEL positive cells in the designated area in the WT control and E13 *GADD45G*$^{-/-}$ embryos. (E) Model for *GADD45G* essential role in midfacial morphogenesis. Loss of *GADD45G* causes continuous cell proliferation, increase in the number of E-cadherin positive cells and suppression of apoptosis in λ and eventually leads to CL. Error bars represent ± SEM. *$p < 0.05$. **$p < 0.01$. $N = 3$ biologically independent samples. Scale bars: 100 μm. (For interpretation of the references to color in this figure legend, the reader is referred to the online version of this chapter.)

(XDA16030501, XDA16030503), and Guangdong Province Science and Technology Plan Project (2014B020225003).

Author contributions

Yi Lu and Zhanjun Li designed research; Zhiquan Liu, Quanjun Zhang and Mingming Liang analyzed data; Yi Lu, Zhanjun Li, Mingming Liang and Yuning Song performed research; Yi Lu, Liangxue Lai and Zhanjun Li wrote the paper; Mingming Liang and Yuning Song contributed new reagents or analytic tools; and all authors have read and approved the final manuscript.

References

[1] L.A. Croen, G.M. Shaw, C.R. Wasserman, M.M. Tolarova, Racial and ethnic variations in the prevalence of orofacial clefts in California, Am. J. Med. Genet. 79 (1998) (1983-1992) 42–47.
[2] M.M. Tolarova, J. Cervenka, Classification and birth prevalence of orofacial clefts, Am. J. Med. Genet. 75 (1998) 126–137.
[3] F.C. Fraser, The genetics of cleft lip and cleft palate, Am. J. Hum. Genet. 22 (1970) 336–352.
[4] M.J. Dixon, M.L. Marazita, T.H. Beaty, J.C. Murray, Cleft lip and palate: understanding genetic and environmental influences, Nat. Rev. Genet. 12 (2011) 167–178.
[5] L.E. Mitchell, K. Christensen, Evaluation of family history data for Danish twins with nonsyndromic cleft lip with or without cleft palate, Am. J. Med. Genet. 72 (1997) 120–121.
[6] T.H. Beaty, M.A. Taub, A.F. Scott, J.C. Murray, M.L. Marazita, H. Schwender, M.M. Parker, J.B. Hetmanski, P. Balakrishnan, M.A. Mansilla, E. Mangold, K.U. Ludwig, M.M. Noethen, M. Rubini, N. Elcioglu, I. Ruczinski, Confirming genes influencing risk to cleft lip with/without cleft palate in a case-parent trio study, Hum. Genet. 132 (2013) 771–781.
[7] S. Birnbaum, K.U. Ludwig, H. Reutter, S. Herms, M. Steffens, M. Rubini, C. Baluardo, M. Ferrian, N. Almeida de Assis, M.A. Alblas, S. Barth, J. Freudenberg, C. Lauster, G. Schmidt, M. Scheer, B. Braumann, S.J. Berge, R.H. Reich, F. Schiefke, A. Hemprich, S. Potzsch, R.P. Steegers-Theunissen, B. Potzsch, S. Moebus, B. Horsthemke, F.J. Kramer, T.F. Wienker, P.A. Mossey, P. Propping, S. Cichon, P. Hoffmann, M. Knapp, M.M. Nothen, E. Mangold, Key susceptibility locus for nonsyndromic cleft lip with or without cleft palate on chromosome 8q24, Nat. Genet. 41 (2009) 473–477.
[8] E. Mangold, K.U. Ludwig, S. Birnbaum, C. Baluardo, M. Ferrian, S. Herms, H. Reutter, N.A. de Assis, T.A. Chawa, M. Mattheisen, M. Steffens, S. Barth, N. Kluck, A. Paul, J. Becker, C. Lauster, G. Schmidt, B. Braumann, M. Scheer, R.H. Reich, A. Hemprich, S. Potzsch, B. Blaumeiser, S. Moebus, M. Krawczak, S. Schreiber, T. Meitinger, H.E. Wichmann, R.P. Steegers-Theunissen, F.J. Kramer, S. Cichon, P. Propping, T.F. Wienker, M. Knapp, M. Rubini, P.A. Mossey, P. Hoffmann, M.M. Nothen, Genome-wide association study identifies two susceptibility loci for nonsyndromic cleft lip with or without cleft palate, Nat. Genet. 42 (2010) 24–26.
[9] T.H. Beaty, J.C. Murray, M.L. Marazita, R.G. Munger, I. Ruczinski, J.B. Hetmanski, K.Y. Liang, T. Wu, T. Murray, M.D. Fallin, R.A. Redett, G. Raymond, H. Schwender, S.C. Jin, M.E. Cooper, M. Dunnwald, M.A. Mansilla, E. Leslie, S. Bullard, A.C. Lidral, L.M. Moreno, R. Menezes, A.R. Vieira, A. Petrin, A.J. Wilcox, R.T. Lie, E.W. Jabs, Y.H. Wu-Chou, P.K. Chen, H. Wang, X. Ye, S. Huang, V. Yeow, S.S. Chong, S.H. Jee, B. Shi, K. Christensen, M. Melbye, K.F. Doheny, E.W. Pugh, H. Ling, E.E. Castilla, A.E. Czeizel, L. Ma, L.L. Field, L. Brody, F. Pangilinan, J.L. Mills, A.M. Molloy, P.N. Kirke, J.M. Scott, M. Arcos-Burgos, A.F. Scott, A genome-wide association study of cleft lip with and without cleft palate identifies risk variants near MAFB and ABCA4, Nat. Genet. 42 (2010) 525–529.
[10] Y. Yu, X. Zuo, M. He, J. Gao, Y. Fu, C. Qin, L. Meng, W. Wang, Y. Song, Y. Cheng, F. Zhou, G. Chen, X. Zheng, X. Wang, B. Liang, Z. Zhu, X. Fu, Y. Sheng, J. Hao, Z. Liu, H. Yan, E. Mangold, I. Ruczinski, J. Liu, M.L. Marazita, K.U. Ludwig, T.H. Beaty, X. Zhang, L. Sun, Z. Bian, Genome-wide analyses of non-syndromic cleft lip with palate identify 14 novel loci and genetic heterogeneity, Nat. Commun. 8 (2017) 14364.
[11] J.M. Salvador, J.D. Brown-Clay, A.J. Fornace Jr., Gadd45 in stress signaling, cell cycle control, and apoptosis, Advances in Experimental Medicine and Biology 793 (2013) 1–19.
[12] M.C. Hollander, A.J. Fornace Jr., Genomic instability, centrosome amplification, cell cycle checkpoints and Gadd45a, Oncogene 21 (2002) 6228–6233.
[13] M. Vairapandi, A.G. Balliet, B. Hoffman, D.A. Liebermann, GADD45b and GADD45g are cdc2/cyclinB1 kinase inhibitors with a role in S and G2/M cell cycle checkpoints induced by genotoxic stress, J. Cell. Physiol. 192 (2002) 327–338.
[14] A. Hoffmeyer, R. Piekorz, R. Moriggl, J.N. Ihle, Gadd45gamma is dispensable for normal mouse development and T-cell proliferation, Mol. Cell. Biol. 21 (2001) 3137–3143.
[15] N. Warr, G.A. Carre, P. Siggers, J.V. Faleato, R. Brixey, M. Pope, D. Bogani, M. Childers, S. Wells, C.L. Scudamore, M. Tedesco, I. del Barco Barrantes, A.R. Nebreda, P.A. Trainor, A. Greenfield, Gadd45gamma and Map3k4 interactions regulate mouse testis determination via p38 MAPK-mediated control of Sry expression, Dev. Cell 23 (2012) 1020–1031.
[16] M.S. Gierl, W.H. Gruhn, A. von Seggern, N. Maltry, C. Niehrs, GADD45G functions in male sex determination by promoting p38 signaling and Sry expression, Dev. Cell 23 (2012) 1032–1042.
[17] H. Johnen, L. Gonzalez-Silva, L. Carramolino, J.M. Flores, M. Torres, J.M. Salvador, Gadd45g is essential for primary sex determination, male fertility and testis development, PLoS One 8 (2013) e58751.
[18] M. Minoux, F.M. Rijli, Molecular mechanisms of cranial neural crest cell migration and patterning in craniofacial development, Development 137 (2010) 2605–2621.
[19] R. Jiang, J.O. Bush, A.C. Lidral, Development of the upper lip: morphogenetic and molecular mechanisms, Developmental Dynamics 235 (2006) 1152–1166.
[20] T.C. Cox, Taking it to the max: the genetic and developmental mechanisms coordinating midfacial morphogenesis and dysmorphology, Clin. Genet. 65 (2004) 163–176.
[21] H.J. Ray, L. Niswander, Mechanisms of tissue fusion during development, Development 139 (2012) 1701–1711.
[22] H. Kurosaka, The roles of hedgehog signaling in upper lip formation, Biomed. Res. Int. (2015) (2015) 901041.
[23] N. Honarpour, C. Du, J.A. Richardson, R.E. Hammer, X. Wang, J. Herz, Adult Apaf-1-deficient mice exhibit male infertility, Dev. Biol. 218 (2000) 248–258.
[24] J.Z. Jin, J. Ding, Analysis of cell migration, transdifferentiation and apoptosis during mouse secondary palate fusion, Development (133) (2006) 3341–3347.
[25] D. Sun, S. Baur, E.D. Hay, Epithelial-mesenchymal transformation is the mechanism for fusion of the craniofacial primordia involved in morphogenesis of the chicken lip, Dev. Biol. 228 (2000) 337–349.
[26] M. Losa, M. Risolino, B. Li, J. Hart, L. Quintana, I. Grishina, H. Yang, I.F. Choi, P. Lewicki, S. Khan, Face morphogenesis is promoted by Pbx-dependent EMT via regulation of Snail1 during frontonasal prominence fusion, Development 145 (2018) dev157628.
[27] H. Kurosaka, A. Iulianella, T. Williams, P.A. Trainor, Disrupting hedgehog and WNT signaling interactions promotes cleft lip pathogenesis, J. Clin. Invest. 124 (2014) 1660–1671.
[28] M. Chen, B. Yao, Q. Yang, J. Deng, Y. Song, T. Sui, L. Zhou, H. Yao, Y. Xu, H. Ouyang, Truncated C-terminus of fibrillin-1 induces Marfanoid-progeroid-lipodystrophy (MPL) syndrome in rabbit, Dis. Model. Mech. 11 (2018) dmm031542.
[29] B. Shen, J. Zhang, H. Wu, J. Wang, K. Ma, Z. Li, X. Zhang, P. Zhang, X. Huang, Generation of gene-modified mice via Cas9/RNA-mediated gene targeting, Cell Res. 23 (2013) 720–723.
[30] Y. Song, L. Yuan, Y. Wang, M. Chen, J. Deng, Q. Lv, T. Sui, Z. Li, L. Lai, Efficient dual sgRNA-directed large gene deletion in rabbit with CRISPR/Cas9 system, Cellular and Molecular Life Sciences, vol. 73, 2016, pp. 2959–2968.
[31] Z. Liu, M. Chen, S. Chen, J. Deng, Y. Song, L. Lai, Z. Li, Highly efficient RNA-guided base editing in rabbit, Nat. Commun. 9 (2018) 2717.
[32] L. Yuan, T. Sui, M. Chen, J. Deng, Y. Huang, J. Zeng, Q. Lv, Y. Song, Z. Li, L. Lai, CRISPR/Cas9-mediated GJA8 knockout in rabbits recapitulates human congenital cataracts, Sci. Rep. 6 (2016) 22024.
[33] S. Bae, J. Park, J.S. Kim, Cas-OFFinder: a fast and versatile algorithm that searches for potential off-target sites of Cas9 RNA-guided endonucleases, Bioinformatics (Oxford, England) 30 (2014) 1473–1475.
[34] V. Metzis, A.D. Courtney, M.C. Kerr, C. Ferguson, M.C. Rondon Galeano, R.G. Parton, B.J. Wainwright, C. Wicking, Patched1 is required in neural crest cells for the prevention of orofacial clefts, Hum. Mol. Genet. 22 (2013) 5026–5035.
[35] T. Sasaki, Y. Ito, P. Bringas Jr., S. Chou, M.M. Urata, H. Slavkin, Y. Chai, TGFbeta-mediated FGF signaling is crucial for regulating cranial neural crest cell proliferation during frontal bone development, Development (133) (2006) 371–381.
[36] J. Iwata, A. Suzuki, R.C. Pelikan, T.V. Ho, P.A. Sanchez-Lara, M. Urata, M.J. Dixon, Y. Chai, Smad4-Irf6 genetic interaction and TGFbeta-mediated IRF6 signaling cascade are crucial for palatal fusion in mice, Development 140 (2013) 1220–1230.
[37] M. Biasini, S. Bienert, A. Waterhouse, K. Arnold, G. Studer, T. Schmidt, F. Kiefer, T. Gallo Cassarino, M. Bertoni, L. Bordoli, T. Schwede, SWISS-MODEL: modelling protein tertiary and quaternary structure using evolutionary information, Nucleic Acids Res. 42 (2014) W252–W258.
[38] A. Gritli-Linde, The etiopathogenesis of cleft lip and cleft palate: usefulness and caveats of mouse models, Curr. Top. Dev. Biol. 84 (2008) 37–138.
[39] A. Gritli-Linde, The mouse as a developmental model for cleft lip and palate research, Frontiers of oral biology 16 (2012) 32–51.
[40] Y. Wang, N. Fan, J. Song, J. Zhong, X. Guo, W. Tian, Q. Zhang, F. Cui, L. Li, P.N. Newsome, J. Frampton, M.A. Esteban, L. Lai, Generation of knockout rabbits using transcription activator-like effector nucleases, Cell regeneration (London, England) 3 (2014) 3.
[41] J. Fan, S. Kitajima, T. Watanabe, J. Xu, J. Zhang, E. Liu, Y.E. Chen, Rabbit models for the study of human atherosclerosis: from pathophysiological mechanisms to translational medicine, Pharmacol. Ther. 146 (2015) 104–119.
[42] T. Sui, L. Yuan, H. Liu, M. Chen, J. Deng, Y. Wang, Z. Li, L. Lai, CRISPR/Cas9-mediated mutation of PHEX in rabbit recapitulates human X-linked hypophosphatemia (XLH), Hum. Mol. Genet. 25 (2016) 2661–2671.
[43] Q. Lv, L. Yuan, J. Deng, M. Chen, Y. Wang, J. Zeng, Z. Li, L. Lai, Efficient generation of myostatin gene mutated rabbit by CRISPR/Cas9, Sci. Rep. 6 (2016) 25029.
[44] J. Deng, M. Chen, Z. Liu, Y. Song, T. Sui, L. Lai, Z. Li, The disrupted balance between hair follicles and sebaceous glands in Hoxc13-ablated rabbits, FASEB J. 33 (2019) 1226–1234.
[45] E. Ferretti, B. Li, R. Zewdu, V. Wells, J.M. Hebert, C. Karner, M.J. Anderson, T. Williams, J. Dixon, M.J. Dixon, M.J. Depew, L. Selleri, A conserved Pbx-Wnt-p63-Irf6 regulatory module controls face morphogenesis by promoting epithelial apoptosis, Dev. Cell 21 (2011) 627–641.
[46] W. Liu, X. Sun, A. Braut, Y. Mishina, R.R. Behringer, M. Mina, J.F. Martin, Distinct functions for Bmp signaling in lip and palate fusion in mice, Development 132

(2005) 1453–1461.
[47] L.L. Brinkley, M.M. Vickerman, The effects of chlorcyclizine-induced alterations of glycosaminoglycans on mouse palatal shelf elevation in vivo and in vitro, Journal of Embryology and Experimental Morphology 69 (1982) 193–213.
[48] J. Okano, S. Suzuki, K. Shiota, Regional heterogeneity in the developing palate: morphological and molecular evidence for normal and abnormal palatogenesis, Congenital anomalies 46 (2006) 49–54.
[49] K. Yu, D.M. Ornitz, Histomorphological study of palatal shelf elevation during murine secondary palate formation, Developmental Dynamics 240 (2011) 1737–1744.
[50] C.K. Miller, Feeding issues and interventions in infants and children with clefts and craniofacial syndromes, Semin. Speech Lang. 32 (2011) 115–126.
[51] M. Kosicki, K. Tomberg, A. Bradley, Repair of double-strand breaks induced by CRISPR-Cas9 leads to large deletions and complex rearrangements, Nat. Biotechnol. 36 (2018) 765–771.
[52] Y. Ma, J. Zhang, W. Yin, Z. Zhang, Y. Song, X. Chang, Targeted AID-mediated mutagenesis (TAM) enables efficient genomic diversification in mammalian cells, Nat. Methods 13 (2016) 1029–1035.
[53] M. Kluesner, D. Nedveck, W. Lahr, J. Garbe, J. Abrahante, B. Webber, B. Moriarity, EditR: A Novel Base Editing Quantification Software Using Sanger Sequencing, bioRxiv, (2017).
[54] L. Teboul, S.A. Murray, P.M. Nolan, Phenotyping first-generation genome editing mutants: a new standard? Mamm. Genome 28 (2017) 377–382.
[55] Y.H. Sung, J.M. Kim, H.T. Kim, J. Lee, J. Jeon, Y. Jin, J.H. Choi, Y.H. Ban, S.J. Ha, C.H. Kim, H.W. Lee, J.S. Kim, Highly efficient gene knockout in mice and zebrafish with RNA-guided endonucleases, Genome Res. 24 (2014) 125–131.
[56] H. Yang, H. Wang, C.S. Shivalila, A.W. Cheng, L. Shi, R. Jaenisch, One-step generation of mice carrying reporter and conditional alleles by CRISPR/Cas-mediated genome engineering, Cell 154 (2013) 1370–1379.
[57] N. Perrimon, Creating mosaics in Drosophila, The International Journal of Developmental Biology 42 (1998) 243–247.
[58] Y.R. Jin, X.H. Han, M.M. Taketo, J.K. Yoon, Wnt9b-dependent FGF signaling is crucial for outgrowth of the nasal and maxillary processes during upper jaw and lip development, Development 139 (2012) 1821–1830.
[59] A.M. Ashique, K. Fu, J.M. Richman, Endogenous bone morphogenetic proteins regulate outgrowth and epithelial survival during avian lip fusion, Development 129 (2002) 4647–4660.
[60] L. Song, Y. Li, K. Wang, Y.Z. Wang, A. Molotkov, L. Gao, T. Zhao, T. Yamagami, Y. Wang, Q. Gan, D.E. Pleasure, C.J. Zhou, Lrp6-mediated canonical Wnt signaling is required for lip formation and fusion, Development 136 (2009) 3161–3171.
[61] A. Lucas, J. Mialet-Perez, D. Daviaud, A. Parini, M.S. Marber, P. Sicard, Gadd45gamma regulates cardiomyocyte death and post-myocardial infarction left ventricular remodelling, Cardiovasc. Res. 108 (2015) 254–267.
[62] A.R. Bassett, C. Tibbit, C.P. Ponting, J.L. Liu, Highly efficient targeted mutagenesis of Drosophila with the CRISPR/Cas9 system, Cell Rep. 4 (2013) 220–228.
[63] H. Wang, H. Yang, C.S. Shivalila, M.M. Dawlaty, A.W. Cheng, F. Zhang, R. Jaenisch, One-step generation of mice carrying mutations in multiple genes by CRISPR/Cas-mediated genome engineering, Cell 153 (2013) 910–918.
[64] K. Nishida, T. Arazoe, N. Yachie, S. Banno, M. Kakimoto, M. Tabata, M. Mochizuki, A. Miyabe, M. Araki, K.Y. Hara, Z. Shimatani, A. Kondo, Targeted nucleotide editing using hybrid prokaryotic and vertebrate adaptive immune systems, Science (New York, N.Y.) 353 (2016).
[65] A.C. Komor, Y.B. Kim, M.S. Packer, J.A. Zuris, D.R. Liu, Programmable editing of a target base in genomic DNA without double-stranded DNA cleavage, Nature 533 (2016) 420–424.
[66] I. Letunic, P. Bork, 20 years of the SMART protein domain annotation resource, Nucleic Acids Res. 46 (2017) D493–D496.
[67] S.A. Brugmann, L.H. Goodnough, A. Gregorieff, P. Leucht, D. ten Berge, C. Fuerer, H. Clevers, R. Nusse, J.A. Helms, Wnt signaling mediates regional specification in the vertebrate face, Development 134 (2007) 3283–3295.
[68] C.R. Ingraham, A. Kinoshita, S. Kondo, B. Yang, S. Sajan, K.J. Trout, M.I. Malik, M. Dunnwald, S.L. Goudy, M. Lovett, J.C. Murray, B.C. Schutte, Abnormal skin, limb and craniofacial morphogenesis in mice deficient for interferon regulatory factor 6 (Irf6), Nat. Genet. 38 (2006) 1335–1340.
[69] T. Rinne, H.G. Brunner, H. van Bokhoven, p63-associated disorders, Cell Cycle (Georgetown, Tex.) 6 (2007) 262–268.
[70] D. Lohnes, M. Mark, C. Mendelsohn, P. Dolle, A. Dierich, P. Gorry, A. Gansmuller, P. Chambon, Function of the retinoic acid receptors (RARs) during development (I). Craniofacial and skeletal abnormalities in RAR double mutants, Development 120 (1994) 2723–2748.
[71] J. Zhang, S. Hagopian-Donaldson, G. Serbedzija, J. Elsemore, D. Plehn-Dujowich, A.P. McMahon, R.A. Flavell, T. Williams, Neural tube, skeletal and body wall defects in mice lacking transcription factor AP-2, Nature 381 (1996) 238–241.
[72] P. Francis-West, R. Ladher, A. Barlow, A. Graveson, Signalling interactions during facial development, Mech. Dev. 75 (1998) 3–28.
[73] Y.A. Kousa, D. Moussa, B.C. Schutte, IRF6 expression in basal epithelium partially rescues Irf6 knockout mice, Developmental Dynamics 246 (2017) 670–681.